may enhance the stability of the resulting complex but are not in themselves sufficient. The dinuclear complexes studied here do not undergo dissociation in polar aprotic solvents, and the incorporation of side chains with potentially diastereotopic protons not only allows the use of ^1H NMR to determine the presence of helicity in the complexes but also improves the solubility of the ligands. The conditions for self-assembly derived from the detailed study of the complexes presented here should be quite general, and we have recently applied them to the successful synthesis of a dinuclear triple helical coordination compound.[41]

Acknowledgment. We gratefully acknowledge support of this research by the Swiss National Science Foundation (Grant No. 21-30139.90).

Supplementary Material Available: A full table of bond distances and angles (Table SI) and details of the extended Hückel calculations (Table SIII) (11 pages); full details in the X-ray structure determination of $[Cu_2(mbzimbe)_2](ClO_4)_2$ in the format of the Standard Crystallographic File Structure[42] (Table SII) (15 pages). Ordering information is given on any current masthead page.

(41) Williams, A. F.; Piguet, C.; Bernardinelli, G. *Angew. Chem., Int. Ed. Engl.* **1991**, *30*, 1490-1492.

(42) Brown, I. D. *Acta Crystallogr., Sect. A* **1985**, *41*, 399.

Electrochemistry and Langmuir Trough Studies of C_{60} and C_{70} Films

Christophe Jehoulet, Yaw S. Obeng, Yeon-Taik Kim, Feimeng Zhou, and Allen J. Bard*

Contribution from the Department of Chemistry and Biochemistry, The University of Texas at Austin, Austin, Texas 78712. *Received November 26, 1991*

Abstract: Thin films of the fullerenes C_{60} and C_{70}, formed by solution casting, were studied by cyclic voltammetry (CV) in MeCN solutions containing quaternary ammonium or alkali-metal salts as supporting electrolytes. The film shows four CV reduction waves and one oxidation wave. The CV behavior for the first reduction, coulometrically equivalent to a one-electron reduction, indicates a large structural reorganization of the film with intercalation of the supporting electrolyte cation and a small amount of dissolution. Upon oxidation of the reduced form, the structure rearranges to form the parent. Similar effects occur for the second reduction/reoxidation process. The size of the cations affects the nature of these CV waves. Scanning electrochemical microscopy (SECM) of the C_{60} films indicates that neither the C_{60} film nor the completely reduced, C_{60}^-, form is a good electronic conductor, while a partially reduced film displays enhanced conductivity. Langmuir trough studies of C_{60} and C_{70} show the preparation of highly incompressible monolayer and multilayer films at the air/water interface. Mixed films of the fullerenes with the surfactant arachidic acid can also be prepared.

Introduction

The electrochemical behavior of thin films of the widely investigated fullerenes such as C_{60}[1,2] is very different than that of the dissolved species. Several studies of the voltammetric behavior of C_{60} and C_{70} dissolved in nonpolar solvents such as benzene, CH_2Cl_2, THF, and dichlorobenzene containing quaternary ammonium salts as supporting electrolyte have appeared.[1a,3-6] Generally the reduction is characterized by a series of reversible cyclic voltammetric (CV) waves representing stepwise one-electron reductions to the anion, dianion, etc.; five such waves have been found for C_{60} in benzene.[6] The general interpretation of these results is that the reduced forms of C_{60} in these solvents and electrolytes, through the pentaanion, are stable and remain soluble on the CV time scale. The oxidation in benzonitrile occurs at quite positive potentials in a multielectron irreversible CV wave, suggesting a complex oxidation reaction sequence and instability of the radical cation.[6]

We recently reported a preliminary study of the CV behavior of thin (~0.1 to 1 μm) films of C_{60} cast on various substrates from C_{60} solutions.[7] These were carried out in acetonitrile (MeCN) solutions containing quaternary ammonium (R_4N^+) or alkali-metal salts in which C_{60} is not appreciably soluble. Although stepwise reduction was also seen with these films, the behavior was considerably more complicated than that found for the dissolved species. For example, there was a large splitting in potential between the reduction and reoxidation waves for the first electron-transfer reaction, which suggested appreciable reorganization of the film during the redox reaction. We also carried out Langmuir trough studies of C_{60}; these revealed the C_{60} films at the air/water interface to be surprisingly stable and highly incompressible.[8] C_{60} also formed stable mixed films with eicosonoic (arachidic) acid. In this study we report a more extensive investigation of the electrochemical behavior of C_{60} films and the first CV experiments with C_{70} films. The use of surface techniques, such as scanning tunneling microscopy (STM), enables us to demonstrate the change of structure of the film during the reduction process. Moreover, it was possible to estimate the relative

(1) (a) Haufler, R. E.; Conceicao, J.; Chibante, L. P. F.; Chai, Y.; Byrne, N. E.; Flanagan, S.; Haley, M. M.; O'Brien, S. C.; Pan, C.; Xiao, Z.; Billups, W. E.; Ciufolini, M. A.; Hauge, R. H.; Margrave, J. L.; Wilson, L. J.; Curl, R. F.; Smalley, R. E. *J. Phys. Chem.* **1990**, *94*, 8634. (b) Krätschmer, W.; Lamb, L. D.; Fostiropoulos, K.; Huffman, D. R. *Nature* **1990**, *347*, 354.

(2) (a) Stoddart, J. F. *Angew. Chem. Int. Ed. Engl.* **1991**, *30*, 70. (b) Diederich, F.; Whetten, R. L. *Angew. Chem. Int. Ed. Engl.* **1991**, *30*, 678. (c) Kroto, H. W.; Allaf, A. W.; Balm, S. P. *Chem. Rev.* **1991**, *91*, 1213 and references therein.

(3) Allemand, P.-M.; Koch, A.; Wudl, F.; Rubin, Y.; Diederich, F.; Alvarez, M. M.; Anz, S. J.; Whetten, R. L. *J. Am. Chem. Soc.* **1991**, *113*, 1050.

(4) Cox, D. M.; Behal, S.; Disko, M.; Gorun, S. M.; Greaney, M.; Hsu, C. S.; Kollin, E. B.; Millar, J.; Robbins, J.; Robbins, W.; Sherwood, R. D.; Tindall, P. *J. Am. Chem. Soc.* **1991**, *113*, 2940.

(5) Dubois, D.; Kadish, K. M.; Flanagan, S.; Haufler, R. E.; Chibante, L. P. F.; Wilson, L. J. *J. Am. Chem. Soc.* **1991**, *113*, 4364.

(6) Dubois, D.; Kadish, K. M.; Flanagan, S.; Wilson, L. J. *J. Am. Chem. Soc.* **1991**, *113*, 7773.

(7) Jehoulet, C.; Bard, A. J.; Wudl, F. *J. Am. Chem. Soc.* **1991**, *113*, 5456.

(8) Obeng, Y. S.; Bard, A. J. *J. Am. Chem. Soc.* **1991**, *113*, 6279.

0002-7863/92/1514-4237$03.00/0

conductivity of the original, totally reduced, or partially reduced (doped) films by scanning electrochemical microscopy (SECM).

We also report Langmuir trough studies of C_{60} and C_{70}, the preparation of Langmuir–Blodgett (LB) films of these alone and mixed with arachidic acid (AA), and preliminary studies of the electrochemistry of LB films. The combined use of all of these techniques produces a more detailed picture of the changes occurring in these films upon reduction and reoxidation.

Thin films of the fullerenes are of interest, because they show interesting properties, such as superconductivity, upon reduction.[9-16] Fullerene-modified electrodes might also find application as sensors or photoelectrochemical (PEC) devices. For example, a recent report[17] confirmed the CV behavior of C_{60} thin films and showed the generation of photocurrents during irradiation of such films in MeCN solutions containing iodide ion. The effect of the cationic counterion (dopant) on the thin film properties is also important. For example, superconductive films are generally formed by sublimation followed by evaporation of an alkali metal (e.g., K, Rb) dopant.[9-16] Studies of such films suggest that only the M_3C_{60}, M_4C_{60}, and M_6C_{60} forms are stable,[18] i.e., that films of the anion and dianion should disproportionate. This seems at odds with the electrochemical behavior of dissolved C_{60} in the presence of R_4N^+; similar studies with alkali-metal ions were not possible because of the insolubility of salts of these in the nonpolar solvents needed to dissolve C_{60}. As discussed in this paper, studies of fullerene films with both R_4N^+ and alkali-metal ions are possible.

Experimental Section

The C_{60} and C_{70} used were either donated by the Wudl group or separated from a commercial carbonaceous soot (Texas Fullerenes Inc., Houston, TX). The purification and chromatographic separation were carried out by the literature method.[3,19] The purity of C_{60} and C_{70} was checked after separation by UV–visible and mass spectroscopy. The electrochemical experiments were conducted in a Vacuum Atmospheres drybox under a helium atmosphere, with different supporting electrolytes [$LiAsF_6$, KPF_6, $NaPF_6$, $CsAsF_6$, and the AsF_6^- salts of TEA^+ (tetraethylammonium), TBA^+ (tetra-*n*-butylammonium), THA^+ (tetra-*n*-hexylammonium), and TOA^+ (tetra-*n*-octylammonium)] and different electrode materials [Au, Pt, glassy carbon (GC)]. The acetonitrile (Burdick & Jackson, Muskegon, MI) was used as received. Adding neutral alumina to the cell did not change the electrochemical behavior, indicating that the water level in the solvent was not sufficient to affect the electrochemical behavior. The supporting electrolytes were purified following the procedures reported previously.[20] The films were prepared by evaporation on the electrode surface of a few microliters of a solution of C_{60} or C_{70} in benzene, dichloromethane, or toluene. Differences between films formed from these solvents will be discussed later.

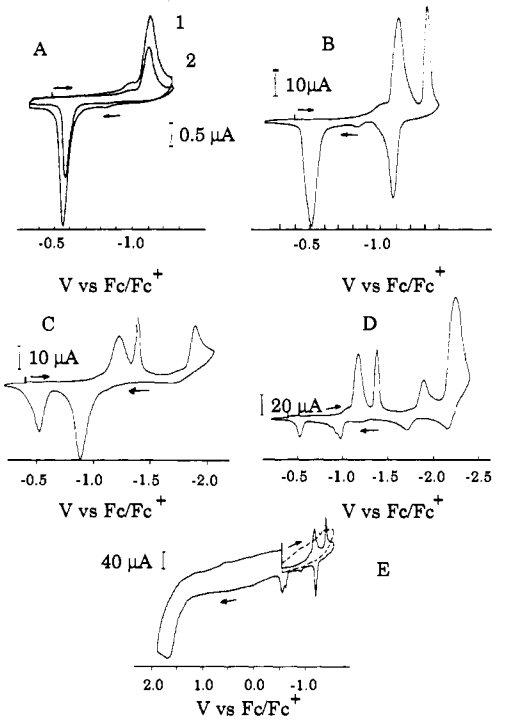

Figure 1. Cyclic voltammograms of C_{60} films on a platinum electrode. Reduction and oxidation reactions on the film: (A and B) First and second reduction processes. Supporting electrolyte, 0.1 M $TBAAsF_6$; scan rate, 200 mV/s (1) and 100 mV/s (2); 250-μm-diameter working electrode. (C, D, and E) Third and fourth reduction and oxidation reactions, respectively. Supporting electrolyte, 0.1 M $TBABF_4$; scan rate, 200 mV/s; 1-mm-diameter electrode. In all CVs, the vertical bar indicates the starting potential and the arrows indicate sweep directions.

In the film balance experiments, arachidic acid (99% ecosonoic acid, Aldrich, Milwaukee, WI) was used as received. Dry benzene and toluene (Spectro grade, Mallinckrodt, Paris, KY) were used as solvents for the preparation of the fullerene spreading solution. Milli-Q water (18 MΩ cm, pH = 6.0, Milli-Q, El Paso, TX) filtered through a 0.5-μm nylon disk (Rainin Instruments, Woburn, MA) was used as a subphase for most of the Langmuir film formation experiments and the Langmuir–Blodgett film transfers. All films were prepared on a Lauda Model P film balance (Brinkman Instruments, Westbury, NY). To form films of the reported limiting molecular areas, 50 μL of a 0.05–0.1 mM solution of C_{60} or C_{70} in benzene ($\sim 3 \times 10^{15}$ molecules) was introduced to the air/water interface by applying the sample in small portions over as large an area as possible and the benzene was then allowed to evaporate for 10–15 min before compression. The trough temperature was regulated by a Lauda Model RM-6 circulator, and films were transferred onto substrates with a Lauda Filmlift.

Cyclic voltammetric experiments were performed with a PAR 173 potentiostat and a PAR 175 universal programmer (Princeton Applied Research Corp., Princeton, NJ). The working electrodes were either Pt (diameter, d, of 250 μm and 1 mm) or Au (d = 250 μm and 2 mm) wires embedded in glass or glassy carbon (GC) (d = 3 mm) in Kevlar. All potentials were measured versus a silver quasi-reference electrode that in turn was calibrated against the ferrocene/ferrocenium (Fc/Fc^+) couple added to the solution. All potentials are reported versus the Fc/Fc^+ couple, which has been taken as 0.31 V vs SCE.[21] Scanning electrochemical microscope (SECM) experiments were performed under a nitrogen atmosphere in a drybox placed over the apparatus. The description of the home-built SECM apparatus has been reported previously.[22] Scanning tunneling microscope (STM) experiments were performed with a Nanoscope II (Digital Instruments, Santa Barbara, CA).

Results: C_{60} Films

Cyclic Voltammetry. Typical voltammograms of C_{60} films in $MeCN/TBAAsF_6$ solutions at a scan rate, v, of 200 mV/s show four reduction peaks on an initial scan to negative potentials, with cathodic peak potentials (E_{pc}) of −1.17, −1.39, −1.88, and −2.24

(9) Haddon, R. C.; Hebard, A. F.; Rosseinsky, M. J.; Murphy, D. W.; Duclos, S. J.; Lyons, K. B.; Miller, B.; Rosamilia, J. M.; Fleming, R. M.; Kortan, A. R.; Glarum, S. H.; Makhija, A. V.; Muller, A. J.; Eick, R. H.; Zahurak, S. M.; Tycko, R.; Dabbagh, G. Thiel, F. A. *Nature* **1991**, *350*, 320.
(10) Zhou, O.; Fisher, J. E.; Coustel, N.; Kycia, S.; Zhu, Q.; McGhie, A. R.; Romanow, W. J.; McCauley, J. P., Jr.; Smith, A. B., III; Cox, D. E. *Nature* **1991**, *351*, 462.
(11) Benning, P. J.; Martins, J. L.; Weaver, J. H.; Chibante, L. P. F.; Smalley, R. E. *Science* **1991**, *252*, 1417.
(12) Holczer, K.; Klein, O.; Huang, S.-M.; Kaner, R. B.; Fu, K.-J.; Whetten, R. L.; Diederich, F. *Science* **1991**, *252*, 1154.
(13) Hebard, A. F.; Rosseinsky, M. J.; Haddon, R. C.; Murphy, D. W.; Glarum, S. H.; Palstra, T. T. M.; Ramirez, A. P.; Kortan, A. R. *Nature* **1991**, *350*, 600.
(14) Tanigaki, K.; Ebbesen, T. W.; Saito, S.; Mizuki, J.; Tsai, J. S.; Kubo, Y.; Kuroshima, S. *Nature* **1991**, *352*, 222.
(15) Kelty, S. P.; Chen, C.-C.; Lieber, C. M. *Nature* **1991**, *352*, 223.
(16) Rosseinsky, M. J.; Ramirez, A. P.; Glarum, S. H.; Murphy, D. W.; Haddon, R. C.; Hebard, A. F.; Palstra, T. T. M.; Kortan, A. R.; Zahurak, S. M.; Makhija, A. V. *Phys. Rev. Lett.* **1991**, *66*, 2830.
(17) Miller, B.; Rosamilia, J. M.; Dabbagh, G.; Tycko, R.; Haddon, R. C.; Muller, A. J.; Wilson, W.; Murphy, D. W.; Hebard, A. F. *J. Am. Chem. Soc.* **1991**, *113*, 6291.
(18) Fleming, R. M.; Rosseinsky, M. J.; Ramirez, A. P.; Murphy, D. W.; Tully, J. C.; Haddon, R. C.; Siegrist, T.; Tycko, R.; Glarum, S. H.; Marsh, P.; Dabbagh, G.; Zahurak, S. M.; Makhija, A. V.; Hampton, C. *Nature* **1991**, *352*, 701 and references therein.
(19) Ajie, H.; Alvarez, M. M.; Anz, S. J.; Beck, R. D.; Diederich, F.; Fostiropoulos, K.; Huffman, D. R.; Krätschmer, W.; Rubin, Y.; Schriver, K. E.; Sensharma, D.; Whetten, R. L. *J. Phys. Chem.* **1990**, *94*, 8630.
(20) Garcia, E.; Kwak, J.; Bard, A. J. *Inorg. Chem.* **1988**, *27*, 4377.
(21) Bard, A. J.; Faulkner, L. R. *Electrochemical Methods*; Wiley: New York, 1980.
(22) Kwak, J.; Bard, A. J. *Anal. Chem.* **1989**, *61*, 1794.

Table I. Peak Potentials and Peak Separation for the First and Second Reduction Processes[a]

	first reduction process				second reduction process			
v, mV/s	E_{pa}, V	E_{pc}, V	ΔE_p, mV	$\Delta E_{p,1/2}$, mV	E_{pa}, V	E_{pc}, V	ΔE_p, mV	$\Delta E_{p,1/2}$, mV
20	−0.72	−1.16	445	50	−1.22	−1.38	160	35
50	−0.69	−1.19	500	65	−1.20	−1.39	190	40
100	−0.66	−1.17	515	80	−1.18	−1.37	190	45
200	−0.63	−1.19	560	85	−1.17	−1.39	220	55
500	−0.58	−1.16	580	95	−1.16	−1.41	250	85

[a] Potentials are referred to the ferrocene redox couple.

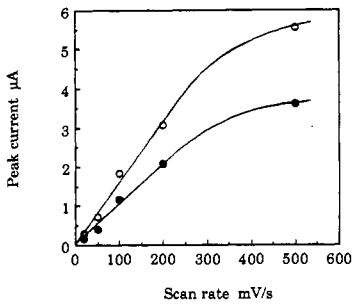

Figure 2. Peak current as a function of scan rate for the first reduction process: (●) reduction; (○) reoxidation.

V vs Fc/Fc^+ and one oxidation peak with an anodic peak potential (E_{pa}) at 1.6 V on an initial scan to positive potentials. Figure 1 shows typical cyclic voltammograms (CV) obtained for a single cycle to different potentials. The effects of continuous cycling will be discussed below. As shown in Figure 1E, no cathodic wave was associated with the oxidative wave of C_{60}. After this wave is scanned, the electroactivity of the film diminished, suggesting the instability of the product of the oxidation reaction. Such an oxidation wave has been recently reported in solution of C_{60} in benzonitrile and was also shown to be irreversible.[6] The film reduction peaks correspond roughly to those observed for dissolved C_{60} in CH_2Cl_2, $C_6H_4Cl_2$, THF, or PhCN and probably represent successive one-electron transfer reactions, as shown for the solution waves.[1a,3-6] For these films the determination by electrolysis of the number of electrons involved in the reduction process was difficult, as the amount of material on the electrode surface was usually not known accurately. However, as shown below, a coulometric experiment shows a one-electron transfer for the first wave.

Behavior of the First and Second Reduction Processes. First Cycle. The electrochemical behavior for a single scan and reversal after the first cathodic wave was different from that observed in solution. Indeed, solution waves were shown to be Nernstian, even at high scan rates (20 V/s).[5,6] In solution, the anodic peaks are located at about the same potentials as the reduction peaks (peak separation, ΔE_p, of about 60 mV).[5,6] Figure 1A,B shows that for the film in TBA^+ solutions the anodic peak was displaced to potentials far positive of the cathodic peak (ΔE_{p1} about 0.5 V for the first wave, ΔE_{p2} about 0.2 V for the second). Table I shows that the peak splitting increases with an increasing scan rate, v. Over the range 20–500 mV/s, the E_{pc} values were essentially independent of v, while E_{pa} shifted toward more positive values by about 140 mV (first peak) and 80 mV (second peak) with increasing v. As expected for a surface wave,[21] the peak current depended linearly on the scan rate, when v was smaller than 200 mV/s (Figure 2). At higher v, i_{pc} and i_{pa} increased more slowly and the peaks broadened, suggesting the onset of kinetic effects on the charge-transfer process. As shown in Table I, the peak widths at half-height were significantly smaller than what is usually observed for a surface-confined species (91 mV per electron).[21] As shown in Figure 1, a pair of small waves between the first main reduction and reoxidation waves was usually also seen. These occurred with all films studied, but with different relative peak heights. As discussed later, similar waves were found with C_{70} films. We assign these waves to a small amount of dissolved C_{60} and C_{60}^-, which results from a slight solubility of the films, especially during the initial scans. This question of film solubility

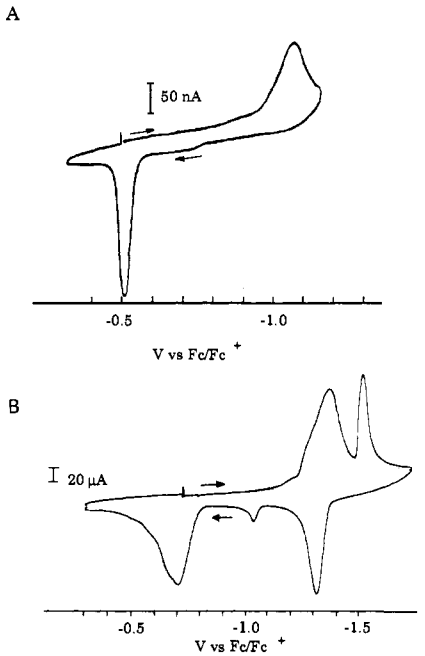

Figure 3. Cyclic voltammograms of C_{60} films: (A) Using 0.1 M TBA-ClO_4 as supporting electrolyte; 250-μm-diameter platinum working electrode; scan rate, 200 mV/s. (B) On a glassy carbon electrode (3-mm diameter) using 0.1 M $TBABF_4$; scan rate, 200 mV/s.

is discussed further in connection with SECM experiments.

To obtain more quantitative coulometric information about the extent of reduction in the film, a known amount of C_{60} contained in 2 μL of a 1 mM solution was dropped on a 3-mm-diameter GC electrode. Under these conditions, all of the C_{60} remained on the electrode with no run off to the surrounding insulator (as happened with the smaller Pt-in-glass electrodes). This amount represented 2.7×10^{-8} mol/cm^2 of C_{60}. If we assume that C_{60} forms a film with a face-centered cubic packing and has a 10-Å diameter,[23-25] a monolayer of C_{60} represents 1.66×10^{-10} mol/cm^2. This sample was therefore equivalent to about 160 layers (about 0.2 μm thickness), if all of the C_{60} molecules were well-packed. However, SECM experiments described below show that the coverage of the electrode before the experiment is rather nonuniform, and formation of small crystallites of C_{60} are expected for films produced by this technique.[25] The charges calculated by integration of the first reduction and reoxidation waves were 2.56 and 2.37 mC/cm^2, respectively. This is only slightly less than that expected for a one-electron reaction (2.7 mC/cm^2). However, smaller amounts of charge were found for the second reduction and reoxidation processes, 1.19 and 1.34 mC/cm^2, respectively. Typically, with many different films, the charge for the second reduction was about 50–70% of that of the first wave (which corresponds roughly to the total amount of C_{60} on the electrode).

(23) David, W. I. F.; Ibberson, R. M.; Matthewman, J. C.; Prassider, K.; Dennis, T. J. S.; Hare, J. P.; Kroto, H. W.; Taylor, R.; Walton, D. R. M. *Nature* **1991**, *353*, 147.
(24) Wilson, R. J.; Meijer, G.; Bethune, D. S.; Johnson, R. D.; Chambliss, D. D.; de Vries, M. S.; Hunziker, H. E.; Wendt, H. R. *Nature* **1990**, *348*, 621.
(25) Wragg, J. L.; Chamberlain, J. E.; White, H. W.; Krätschmer, W.; Huffman, D. R. *Nature* **1990**, *348*, 623.

Very similar results were obtained for different electrode materials (Pt, Au, or GC) and with different counteranions in the TBA^+ supporting electrolyte (ClO_4^-, PF_6^-, BF_4^-, AsF_6^-) (Figure 3). This large peak splitting between the anodic reversal wave and the cathodic wave resembles the behavior already observed (although with smaller splitting magnitudes) in the CV of TTF-TCNQ pellets[26,27] or TTFBr in films or in Nafion layers on electrodes.[28] In that case, the behavior was attributed to large structural rearrangements of the film following the electron transfer. Therefore, the following scheme is proposed for the first reduction:

$$\begin{array}{ccc} (C_{60})_A + TBA^+ + e^- & \rightleftharpoons & (C_{60}^-\cdot TBA^+)_A \\ \uparrow & & \downarrow \\ (C_{60})_B + TBA^+ + e^- & \rightleftharpoons & (C_{60}^-\cdot TBA^+)_B \end{array}$$

where A and B represent different film structures.

Upon reduction, most of the material is reduced to C_{60}^-; TBA^+ ions diffuse into the film to balance the negative charges. Before the reduction, the film consists of C_{60} crystallites, each packed in the face-centered cubic (fcc) mode.[23] TBA^+, which has a size close to that of the C_{60} molecule, cannot intercalate into the spaces of the fcc structure. Therefore, the system rearranges to a new, more stable, configuration. This structural change is supported by scanning tunneling microscopy studies discussed below. After reoxidation, TBA^+ leaves the film and the C_{60} rearranges to its initial structure. Thus, upon reduction and reoxidation the film should expand and contract allowing the structure to become more ordered. The CV behavior indicates that the rates of both rearrangements are high, as no anodic peaks were observed at potentials close to the reduction peak potentials. However, scans could only be performed for scan rates up to 1 V/s, because broadening of the peaks occurs at higher scan rates. Note, as discussed in connection with the SECM experiments, both the C_{60} and $TBA^+C_{60}^-$ films were not good electronic conductors, so that the wave shapes are perturbed to some extent by resistance (iR) effects. These are more important at high sweep rates where high currents flow. Intuitively, the mechanism for the second reduction wave should be similar to that for the first reduction. However, the splitting for the second pair of waves was smaller than for the first reduction process and the charge put into the film was also 50–70% of the charge measured for the first reduction.

Continuous Cycling. The changes in the CV upon continuous cycling over the first reduction/reoxidation waves or over both the first and the second reduction/reoxidation waves are displayed in Figure 4. The current first increased slightly during the first few cycles. This can be explained by the fact that during the first scan a small amount of C_{60} (about 5%) on the electrode was not reduced. The rearrangement occurring during the first cyclic scan apparently improves the uniformity and accessibility of the film on the electrode. This also allows the release of the molecules of solvent (benzene, toluene, or dichloromethane) trapped during the evaporation process. There was usually a small shift in the reduction peak potential between the first cycle and the second cycle and a change in the shape of the peaks for the first reduction. This was especially seen when the film was formed from a solution of C_{60} in toluene. The difference in the shape of the peaks between the first and second cycle was then more pronounced compared to films cast from benzene solutions. This suggests that toluene is more easily trapped in the C_{60} crystallites as previously reported.[29] After a few cycles, the peak currents began to decrease until eventually no electrochemical activity was observed. This process could take 2–3 h for a 3-mm-diameter electrode. This time to inactivation upon extended cycling depended strongly on

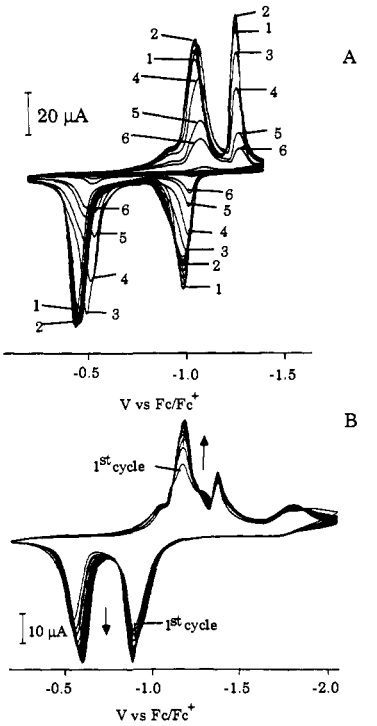

Figure 4. Effect of continuous cycling on C_{60} films on a 1-mm-diameter platinum electrode. Supporting electrolyte, 0.1 M $TBAAsF_6$; scan rate, 200 mV/s. (A) Cycling over the first reduction process: (1) first cycle; (2) after 10 cycles; (3) after 5 min; (4) after 10 min; (5) after 20 min; (6) after 25 min. (B) Cycling over the third reduction process.

the total amount of material on the surface and on the size of the electrode. Smaller electrodes became inactive much faster. One explanation of this deactivation upon cycling is loss of porosity of the film. As shown by the scanning electrochemical microscopy (SECM) experiments (discussed below) both C_{60} and $TBA^+C_{60}^-$ are quite resistive. Thus reduction and reoxidation depend upon accessibility of all parts of the film to TBA^+ and solvent. With cycling, if the film becomes more compact, loses contact to the underlying electrode material, or loses interparticle contact, then less and less of the C_{60} material remains available for reduction and oxidation. The loss of electroactivity after extensive cycling is not due to loss of material by flaking off from the electrode surface or by complete dissolution. Indeed, SECM experiments demonstrate the presence of a resistive film on the electrode after a continuous cycling process.

The doping of the film could also be studied by holding the potential just beyond the first reduction wave of C_{60}. In this case, the electrochemical activity of the film was suppressed more rapidly than in a continuous cycling process. But, as in the previous case, the loss of electroactivity cannot be explained by loss of material from the electrode or complete dissolution of the film, as shown by the following voltammetric experiments with a dissolved species (Fc). Such experiments are frequently used to test the porosity of electronically insulating films on electrode surfaces,[30] since the oxidation of Fc can occur at exposed or available Au sites. Note that the oxidation of Fc occurs at potentials where no redox process of C_{60} occurs (Figure 5A). The CV on an electrode with a C_{60} film is shown in Figure 5A. At this scan rate the CV is only slightly perturbed from that at the bare electrode, because the diffusion layer resulting from electrolysis in the pores of the film has sufficient time to build up to encompass the whole (geometric) area of the electrode. In general, for a porous film, $i_p/v^{1/2}$ shows a characteristic behavior as a function of v. At low scan rates, $i_p/v^{1/2}$ is constant and close to the value expected for a bare electrode. At high scan rates, the diffusion layer is restricted to an area very close to that of the

(26) Jaeger, C. D.; Bard, A. J. *J. Am. Chem. Soc.* **1979**, *101*, 1690.
(27) Jaeger, C. D.; Bard, A. J. *J. Am. Chem. Soc.* **1980**, *102*, 5435.
(28) Henning, T. P.; Bard, A. J. *J. Electrochem. Soc.* **1983**, *130*, 613.
(29) Milliken, J.; Keller, T. M.; Baronavski, A. P.; McElvany, S. W.; Callahan, J. H.; Nelson, H. H. *Chem. Mater.* **1991**, *3*, 386.
(30) Amatore, C.; Savéant, J. M.; Tessier, D. *J. Electroanal. Chem.* **1983**, *147*, 39.

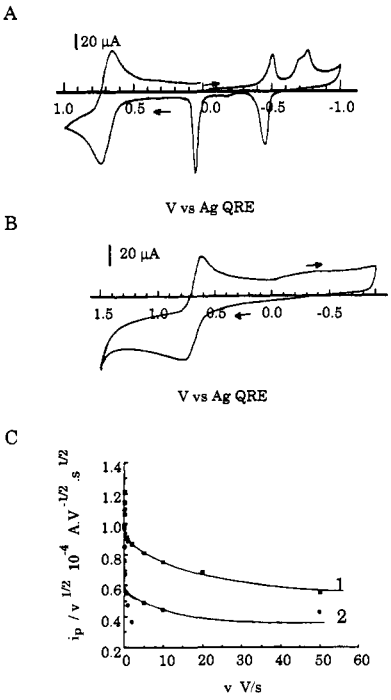

Figure 5. (A) Cyclic voltammogram of C_{60} films on a 2-mm-diameter gold electrode in a 2 mM Fc/0.1 M $TBAPF_6$/MeCN solution at $v = 0.2$ V/s: (A) before reduction of the film; (B) after reduction of the film (potential held after the first reduction wave for 1.5 h); (C) $i_p/v^{1/2}$ as a function of scan rate for Fc/Fc^+ (1) before any scan over the C_{60} reduction peak and (2) after total reduction of the film (as in B).

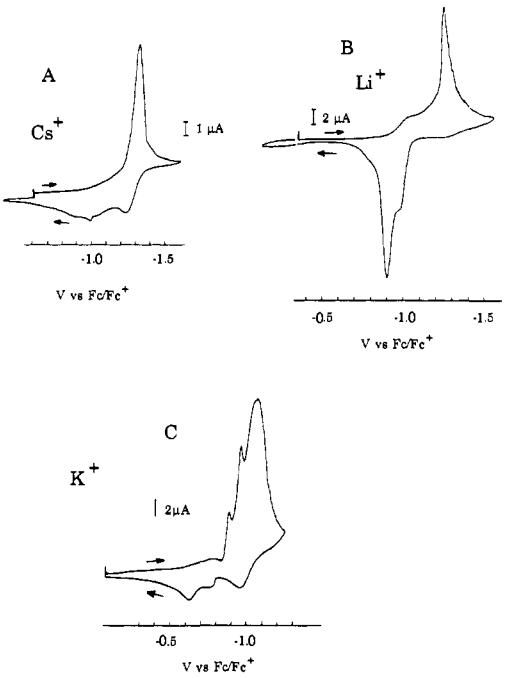

Figure 6. Cyclic voltammograms of C_{60} films on metal electrodes using various supporting electrolytes: (A) 0.1 M $CsAsF_6$ with a 250-μm-diameter platinum electrode; (B) 0.1 M $LiAsF_6$ with a 250-μm-diameter gold electrode; (C) 0.1 M KPF_6 with a 1-mm-diameter platinum electrode. Scan rate, 200 mV/s.

pores and therefore $i_p/v^{1/2}$ is characteristic of the active (exposed) area of the electrode, which is much smaller than the geometric area. Figure 5C shows the decrease of $i_p/v^{1/2}$ as a function of scan rate, which demonstrates the porosity of the film and the inactivity of the C_{60} surface itself for Fc oxidation. For the initial film, the active area was about 46% of the geometric area. Similar experiments with the totally reduced film also show the presence of a porous inactive film on the Au substrate. In this case, $i_p/v^{1/2}$ was even lower, showing a decrease in the porosity of the film as it changed from the C_{60} structure to the totally reduced $TBA^+C_{60}^-$ structure (active area about 35% of the geometric one).

Effect of the Nature and Size of the Supporting Electrolyte Cation. The mechanism proposed for the first reduction and reoxidation reactions suggests that the nature and size of the cation should have an effect on the rearrangement process. Indeed, smaller cations should be intercalated more easily into the spaces of the lattice formed by the C_{60} molecules. Figure 6 shows the electrochemical behavior of C_{60} films in the presence of different cations. The overall behavior described here was observed in many different sets of experiments with both C_{60} samples and supporting electrolyte salts from various origins. When the size of the cation (Na^+, K^+, Cs^+, or TEA^+) was significantly smaller than the size of C_{60}, the CV obtained was quite different than that observed for larger cations than TBA^+ (THA^+ or TOA^+). For small cations (TEA^+, Cs^+, K^+), the CV was characterized by a large reduction wave whose potential was close to that observed for TBA^+ (−1.12 V vs Fc for TEA^+, −1.07 V for K^+, −1.33 V for Cs^+, −1.26 V for Li^+). However, the anodic part of the scan on reversal was very different than that of the C_{60}/TBA^+ system. Indeed, with smaller cations, the overall charge passed in reoxidation was small (about 40%) compared to the charge passed in reduction (about 95% of the charge expected for a one-electron reduction of the film). Moreover, two anodic peaks were usually observed following reversal after the single reduction peak. For Cs^+ (Figure 6A) and K^+ (Figure 6B) a small anodic peak occurred at potentials near the cathodic peak, in addition to an oxidation at more positive potentials. However, with Li^+ the behavior was closer to that found with TBA^+. The difference in behavior of Cs^+ and K^+ vs TBA^+ may indicate differences in structure and chemistry of the C_{60} films. Indeed, recent studies suggest that there is no stable structure between solid C_{60} and solid M_3C_{60} (M = K, Rb, Cs).[18] This would imply that in this case the reduction would be an overall three-electron reaction, e.g., that the formation of any $K^+C_{60}^-$ would be followed by a disproportionation of that compound to the C_{60}^{3-} form.

The peak splitting between the cathodic peak and the more positive anodic wave, when it could be observed, was generally smaller with smaller cations than for the C_{60}^-/TBA^+ films (330 mV for Cs^+, 400 mV for TEA^+; 450 mV for K^+, 360 mV for Li^+ compared to 560–600 mV for TBA^+ at similar scan rates). The reduced films obtained for small cations also appeared less stable than the ones obtained with TBA^+; after 10 or fewer cycles, the electrochemical activity of the film had disappeared. However, as with $TBA^+C_{60}^-$, the films were still on the electrode surface. This was checked qualitatively by recording the CV of benzoquinone added to the solution after cycling over the first reduction and reoxidation wave of C_{60} until no electroactivity was detected. The CVs of BQ showed that the films were still present on the electrode, with the behavior depending on the size of the cation of the supporting electrolyte (Figure 7). The results again suggest the presence of a largely electroinactive, nonconductive, porous film on the electrode surface.

The behavior observed for larger cations (TOA^+) is closer to the behavior of the C_{60}/TBA^+ system (Figure 8). The first and second reduction peaks were obtained at −1.04 and −1.39 V vs Fc, respectively, with a splitting between reduction and reoxidation peaks of about 520 and 250 mV for the first and second electron-transfer processes. These values are close to that observed for the C_{60}/TBA^+ system. However, there were some differences in the electrochemical behavior compared to that of TBA^+. Upon cycling, if the potential was scanned over the first pair of waves, the peak currents decreased to a steady-state value within 5–10 min (Figure 8A). Then, the second reduction and reoxidation peaks were much broader and charges calculated from integration of the CV waves show that the second reduction involves more charge relative to the first wave than in the TBA^+/MeCN solutions. The ratio (Q_{r2}/Q_{r1}) of the charges calculated for the first and second processes (Q_{r1} and Q_{r2}, respectively) was 1.5 for TOA^+/MeCN solutions compared to 0.6 for TBA^+/MeCN solutions.

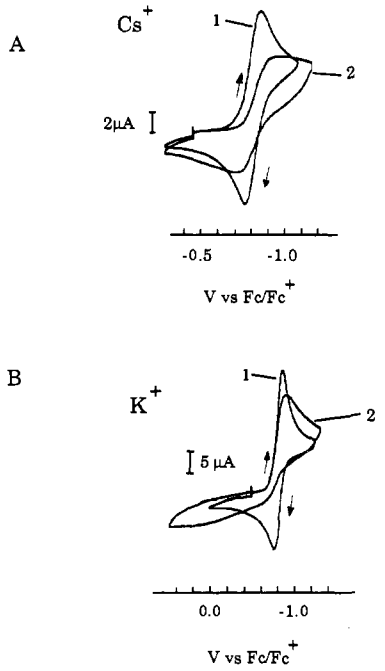

Figure 7. Cyclic voltammograms of benzoquinone in MeCN solution with different supporting electrolytes: (A) 0.1 M $CsAsF_6$; (B) 0.1 M KPF_6. Curve 1 represents the bare electrode. Curve 2 represents the electrode covered with a totally reduced film. Scan rate, 200 mV/s; 1-mm-diameter platinum working electrode.

When the potential was scanned over the second reduction process, the anodic wave associated with the first electron transfer increased on the reverse scan (Figure 8B). However, after this scan, the peak currents of the first reduction process recovered their initial value (Figure 8C).

Further Reductions. Two other reduction processes are observed for TBA^+/C_{60} films in MeCN. As shown in Figure 1, scans over the third and fourth reduction waves resulted in reoxidation waves on scan reversal that were different than the ones observed for reversal past the first and second reduction waves. Indeed, if the potential was scanned over the third reduction, no specific reoxidation wave was associated with that reduction, and the significant modification of the second and first reoxidation waves suggested decomposition of the product of this third reduction (Figure 4). Moreover, when the potential was held just beyond the third reduction wave, the film slowly came off the electrode. Scanning the potential over the fourth reduction wave irreversibly damaged the film, as all of the reduction peaks essentially disappeared on the following scan. The fourth reduction peak was significantly larger than the previous waves, indicating an irreversible multiple-electron transfer. The differences between the experiments on the various reduced states of the films, either by continuous cycling or by holding the potential, indicate that the solubility and the reactivity of the reduced forms of C_{60} increase with their degree of reduction.

Scanning Tunneling Microscopy (STM) of Films. The STM image of a film of C_{60} cast from a CH_2Cl_2 solution on a gold evaporated on mica substrate (Figure 9A) showed that the film was not uniform. However, individual, spherical C_{60} molecules, presumably on the top layers of the film, could be seen. Their diameter was 10.5 ± 0.5 Å as previously reported in STM studies of C_{60} films.[24,25] It was not possible to observe a good STM image of the reduced form of the film following electrochemical reduction in $TBABF_4$/MeCN, probably because these thick films were too resistive. We had better results showing the effect of reduction on thin films transferred by the LB technique. An image of a C_{60} film on I_2-modified single-crystal Pt(111) shows individual C_{60} molecules, in an uneven distribution (Figure 9B). When this filmed electrode was reduced in a $TBABF_4$/MeCN solution, reduction of I_2 to I^- occurred (as seen from the CV response), but the film remained on the electrode. Reduction of this film ex situ

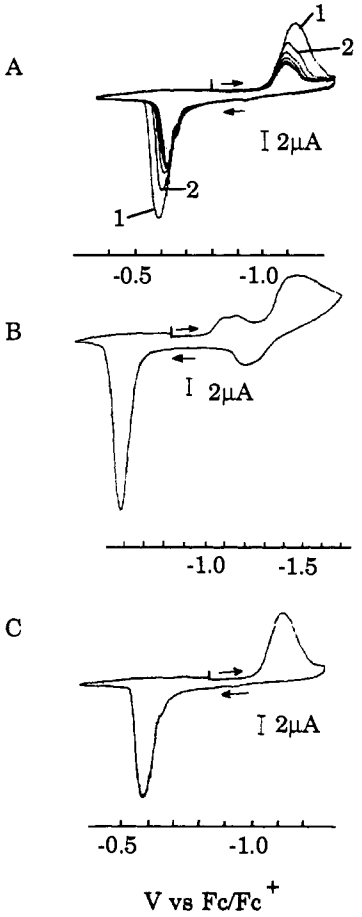

Figure 8. Cyclic voltammogram of a film of C_{60} on a 250-μm-diameter platinum electrode in a 0.1 M $TOAAsF_6$/MeCN solution: (A) continuous cycling; (B) second reduction; (C) first reduction. The CVs were recorded in the order shown here. Scan rate, 200 mV/s.

in $TBABF_4$/MeCN showed a change in the structure of the film (Figure 9D). Individual C_{60} molecules could not be seen and the structure consisted of larger clumps.

Scanning Electrochemical Microscopy. Scanning electrochemical microscopy experiments (SECM) were conducted to obtain an in situ image of the topography of the film as well as information about its porosity and conductivity as a function of the extent of reduction. In SECM, an ultramicroelectrode tip (radius, a, ~1–25 μm) is moved in close proximity to a surface under investigation.[31-33] The effect of the surface (in this case, the C_{60} film) on the magnitude of the tip faradaic current (termed "feedback") provides information about the conductivity and rates of heterogeneous reactions on the film. For an insulating substrate, the observed steady-state tip current (i_T) is smaller than $i_{T,\infty}$ (where $i_{T,\infty}$ is the steady-state current with the tip far from the substrate surface) ("negative feedback"). When the substrate is conducting, the tip-generated product can be electrolyzed and $i_T > i_{T,\infty}$ ("positive feedback"). In these experiments a drybox was placed over the SECM apparatus to allow the use of a deaerated $TBABF_4$/MeCN mixture, as in the previous CV experiments. The distance between the tip and the substrate was estimated by using tetramethyl-*p*-phenylenediamine (TMPD) as a mediator.

As before, the C_{60} films were cast onto Pt or Au substrate surfaces by evaporation of a few microliters of a C_{60}/benzene solution. An image of a Au electrode covered with a C_{60} film is shown on Figure 10A. The film at the electrode surface was not

(31) Bard, A. J.; Fan, F.-R. F.; Kwak, J.; Lev, O. *Anal. Chem.* **1989**, *61*, 132.
(32) Bard, A. J.; Denuault, G.; Lee, C.; Mandler, D.; Wipf, D. O. *Acc. Chem. Res.* **1990**, *23*, 357.
(33) Bard, A. J.; Fan, F.-R. F.; Pierce, D. T.; Unwin, P. R.; Wipf, D. O.; Zhou, F. *Science* **1991**, *254*, 68.

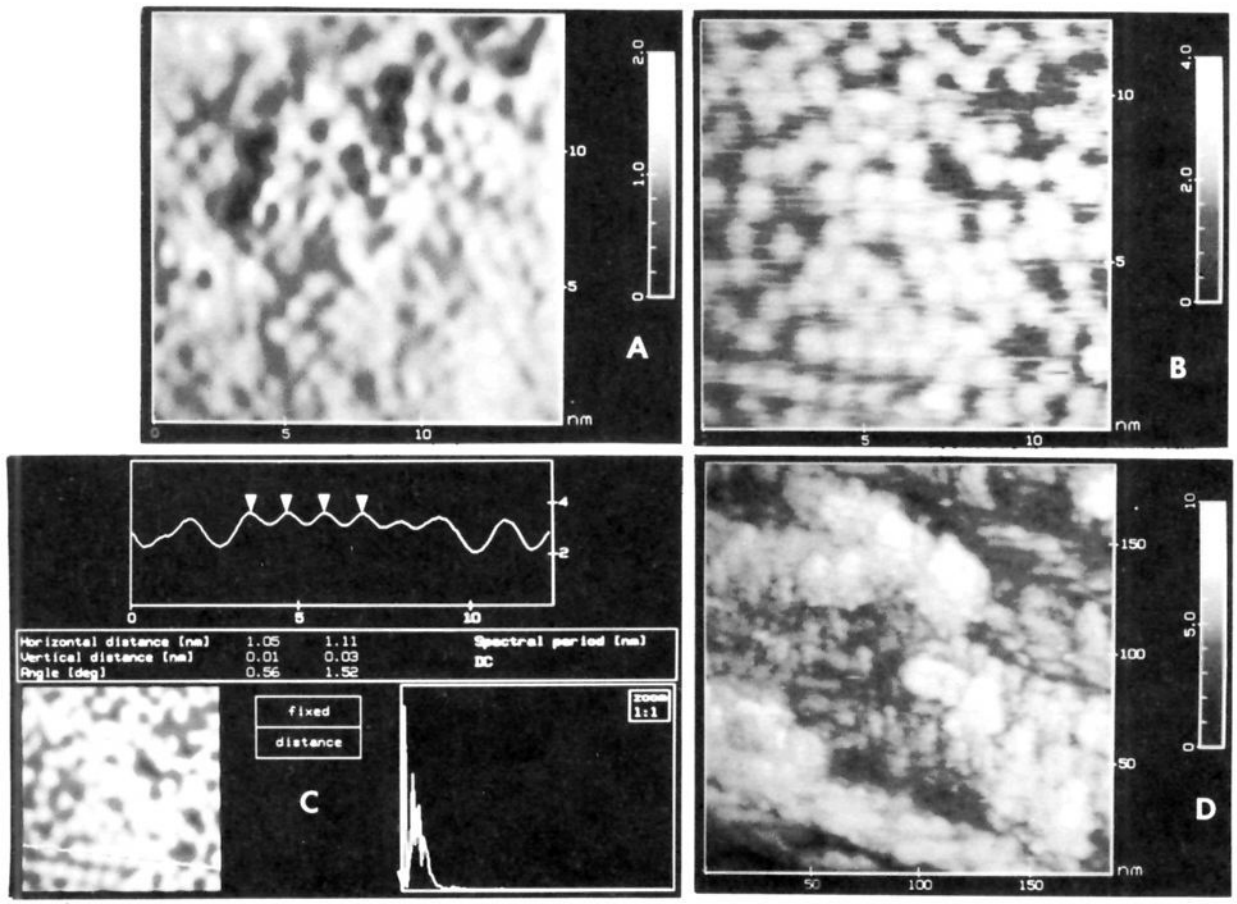

Figure 9. Scanning tunneling microscope images of C_{60} films. (A) Film cast by evaporation of a C_{60}/dichloromethane solution. (B) LB films on I_2/Pt(111) electrode. (C) Close-up of the previous image and depth profile. Estimation of the distance between the centers of the molecules. (D) Same as (B) after reduction ex situ. The electrode was rinsed in MeCN before imaging. Imaging conditions: (A) V_b = 500 mV, i_t = 0.26 nA; (B) V_b = −325 mV, i_t = 0.51 nA; (C) V_b = −1 V, i_t = 2.8 nA. The scanned area was 400 × 400 nm.

uniform. The feedback current was smaller than $i_{T,\infty}$ in most locations, suggesting that the C_{60} film is not conductive, i.e., that $TMPD^+$ generated at the tip was not reduced to TMPD on the C_{60} surface. Positive feedback corresponding to rapid reduction of $TMPD^+$ is observed on bare Au surfaces and some areas of the filmed electrode displayed a positive feedback current, demonstrating that the Au surface was not completely covered by C_{60} and that the film was rather porous. Figure 10B shows another area of the surface that showed a higher i_T ($>i_{T,\infty}$) over most of the area, indicating greater film porosity. Note that some areas of the film showed very low currents, showing large pieces of relatively nonporous material.

In another experiment, images were recorded at the boundary between a Au electrode and the insulating glass surrounding the Au (located at about the 100-μm mark in Figure 11A), with a film of C_{60} covering both Au and glass, to obtain information about film conductivity during reduction. A scan of the original C_{60} film showed clearly the boundary between the film-covered Au and the film-covered glass (Figure 11A). The film in this case was clearly quite porous and not very uniform, as significant positive feedback was observed in the Au region. Over the insulating glass covered with C_{60}, $i_T < i_{T,\infty}$ confirming that C_{60} films were not conductive. The film was then reduced completely by continuously cycling the potential over the first reduction and reoxidation waves until no electroactivity was seen. In a SECM scan the tip current over the substrate was smaller than that of the unreduced C_{60} but still displayed some positive feedback. Moreover, the reduced film appeared more uniform. Negative feedback was still observed over the insulating region. We conclude from this experiment that neither the original C_{60} film nor the completely reduced film after extended cycling over the first reduction wave was conductive and that the reduced form was more uniform and less porous than the original film.

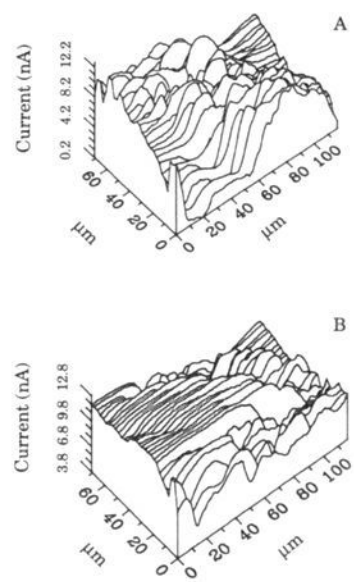

Figure 10. SECM image of a C_{60} film on a gold electrode at open circuit before any electrochemical experiments at two different locations. Solution, MeCN containing 0.1 M $TBABF_4$ and 5.8 mM TMPD; tip, 5-μm-diameter platinum; $i_{T,\infty}$ = 11.8 nA.

However, similar SECM experiments indicated that a partially reduced film was more conductive. This experiment was performed with a Pt substrate surrounded by a Teflon sheath, both covered with a C_{60} film (Figure 11C). In these scans, the tip was

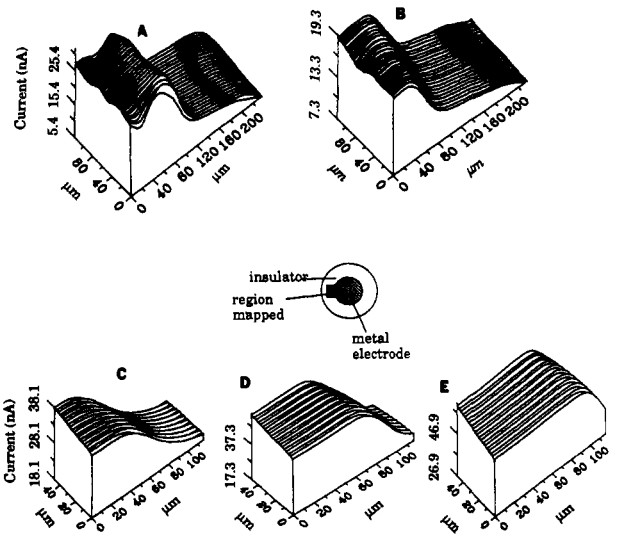

Figure 11. SECM image of a film on a gold electrode at the gold/glass boundary in MeCN with 0.1 M $TBABF_4$ and 0.76 mM TMPD. (A) Before electrochemical experiment. (B) Reduced film. Tip, 25-μm-diameter platinum; $i_{T,\infty}$ = 14.5 nA. SECM image of a film on a platinum electrode at the platinum/Teflon boundary in MeCN with 0.1 M $TBABF_4$ and 1.8 mM TMPD. The potential was held after the first reduction wave of C_{60}. (C) Before electrochemical experiment, (D) after 10 min; (C) after 35 min. Tip, 25-μm-diameter platinum; $i_{T,\infty}$ = 30.7 nA.

not as close to the substrate as in the previous experiments, so small features were not distinguished on the film over the Pt part of the substrate. As in the earlier experiments, before electrochemical reduction of the film, the portion over the Pt part displayed a positive feedback current showing porosity of the film, while that over the Teflon was clearly insulating (boundary at ~80 μm). The potential of the substrate was then held at a value just beyond the first reduction peak for various lengths of time. The tip current recorded over the Pt surface increased significantly, indicating an increase in the conductivity of the film when partially reduced (Figure 11D). Moreover, the current over the Teflon region near the Pt also displayed positive feedback, demonstrating conductivity of the partially doped film extending over the insulating region. Further reduction caused an additional increase in the feedback current and a greater extension of positive feedback into the Teflon region (Figure 11E). However, as before, on extensive reduction, the current over the Pt region dropped, and the film characteristics were those of a porous, nonconductive material. This experiment indicates that the partially reduced (partially TBA^+ doped) C_{60} film is somewhat conductive.

The final SECM experiment was performed to determine the possibility of solubility of C_{60}^- in acetonitrile (Figure 12). This experiment was carried out in the generation/collection mode,[31] with the tip held at a potential where solution mediator (Fc) oxidation did not occur. The mediator was added to the solution to permit positioning of the tip close to the substrate covered by the C_{60} film. The potential of the substrate was cycled over the first reduction wave while the tip potential was held positive to the C_{60}^- reoxidation wave (0.3 V vs AgQRE). In this case, any C_{60}^- produced on the substrate and soluble in MeCN will be detected by the tip.

In the first scan over the first reduction wave, anodic current is indeed found at the tip (Figure 12A). The delay between the onset of cathodic current on the substrate and anodic current at the tip is caused by the time needed for soluble product to cross the substrate/tip gap. However, most of the material remains on the electrode surface. Later cycles over the same region (Figure 12B) show essentially no tip current, suggesting that, with cycling, a less soluble $TBA^+C_{60}^-$ is formed or that the initial material contained residual solvent from the casting procedure that affected film solubility. Films cast from benzene showed similar behavior with higher currents at the tip during C_{60} film reduction. This

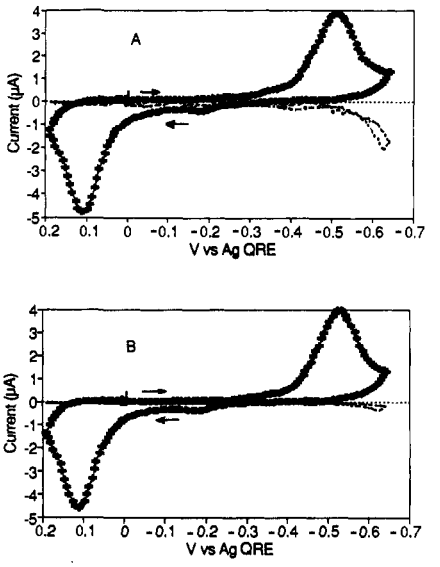

Figure 12. (A) SECM image of a C_{60} film on a 1-mm-diameter gold electrode. (-+-) Substrate current. Cycle over the first pair of waves. (---) Tip current. The potential of the tip was held at 0.3 V vs AgQRE. Solution, 0.1 M $TBAPF_6$ and 10 mM Fc; tip, 10-μm-diameter platinum. The film was cast from a C_{60}/CH_2Cl_2 solution. (B) Same as (A) after 10 cycles over the first pair of waves.

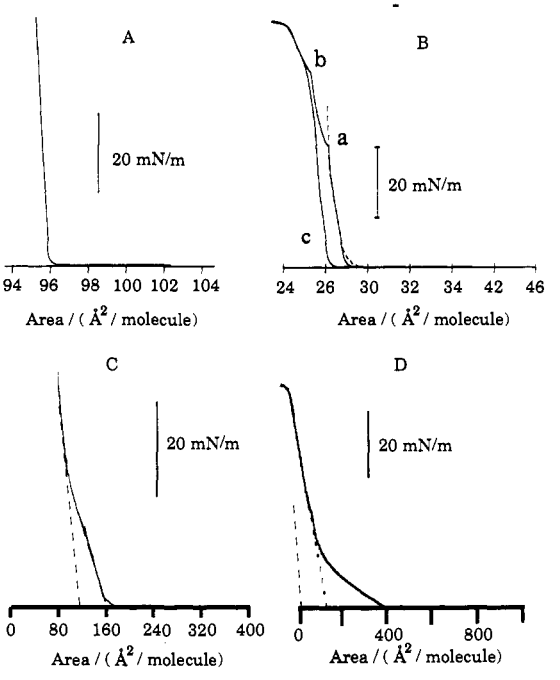

Figure 13. Pressure/area (Π–A) isotherms of (A) pure C_{60} and (B) 1:1 C60/AA mixed films on water (Milli-Q) at 25 °C. (a) Arachidic acid during the initial compression; (b) mixed film during the initial compression; (c) same as (b) after $^1/_2$ h relaxation at Π < 1 mN/m. Subsequent relaxation and recompression cycles followed (c). Pressure/area isotherm of (C) pure C_{70} and (D) 1:1 C_{70}/AA mixed films on water (Milli-Q) at 25 °C.

higher solubility suggests that residual solvent in the film may be important in the dissolution effects observed and is consistent with a somewhat greater affinity of C_{60} for benzene than for CH_2Cl_2.

Langmuir Films of C_{60}. Since C_{60} is insoluble in water, films of C_{60} alone, or mixed with a typical surfactant, could be formed at the air/water interface on a film balance.[8] Figure 13A shows typical Π–A isotherms for neat films of C_{60} formed as described in the Experimental Section. The fully compressed fullerene monolayer films were remarkably rigid and sustained high surface pressures (Π > 65 mN/m); such films could be maintained at a pressure of 35 mN/m for more than 2 h without any noticeable

area loss. The C_{60} films show a single transition in their Π–A isotherm, which probably represents the transformation of the film from a network of monomolecular thick rafts into a coherent monolayer. The limiting area per molecule calculated from Figure 13A yielded a radius of 5.6 ± 0.7 Å for C_{60}. This radius is in good agreement with STM and X-ray powder diffraction studies.[24,25,34] The attainment of reproducible results for pure C_{60} films was very dependent on the mode of application of the material onto the air/water interface.[35] The dilute C_{60} solution had to be spread slowly over a large surface area in tiny drops, never allowing the solution to accumulate at the interface (see under Experimental Section). Any deviation from this protocol resulted in films that collapsed to produce bi- or multilayers. The addition of larger sample portions to the water surface would produce small yellow crystallites, rather than insoluble monolayer rafts, and these crystallites produced multilayers on compression. Such multilayers were even more rigid than the monolayers and could sustain $\Pi > 100$ mN/m for 8 h; smaller apparent limiting molecular radii (~3.5 Å) were found with these multilayer films.

The C_{60} molecules also formed stable mixed films with eicosonoic (arachidic) acid (AA) at the air/water interface (Figure 13B). For films where the ratio $[AA]/[C_{60}] = 1$ in the spreading solution, the average limiting molecular area was ~28 Å^2/molecule of AA (Figure 13B). This is the same limiting area as that found for AA films alone, suggesting that, at high pressures, the C_{60} molecules are squeezed off of the water surface. Similar observations were previously made with mixed films containing molecules of very different sizes, e.g., mixed films of stearic acid and tri-*p*-cresyl phosphate, where the smaller molecules determined the limiting area at high pressures.[36] The C_{60} was probably pushed off of the air/water interface into the more hydrophobic environment created by the packed hydrocarbon tails of the AA molecules, consistent with the known hydrophobicity of C_{60}. The presence of C_{60} in the hydrophobic regions of the compact AA films increased the strength of the resultant composite films. While pure AA films collapsed at ~45 mN/m, the mixed films routinely survived $\Pi > 70$ mN/m (Figure 13B). In contrast to the pure C_{60} films, which showed no hysteresis in their Π–A isotherms on relaxing and recompression, the mixed films showed significant hysteresis when expanded from $\Pi > 40$ mN/m (Figure 13B, curves b and c). These C_{60} film properties were essentially the same over the temperature range studied (5–35 °C) as well as with other subphases, such as 0.1 M KCl and 0.2 M Na_2SO_4.

Langmuir–Blodgett Films of C_{60} and Their Electrochemical Behavior. After the characterization of thin films of C_{60} by Langmuir trough studies, we attempted to transfer these films to electrode surfaces using the vertical lift or horizontal touch techniques to study their electrochemical behavior and compare it to that of thicker films. It was not possible to transfer coherent monolayer Langmuir–Blodgett (LB) films of C_{60} onto a variety of substrates, e.g., freshly cleaved highly oriented pyrolytic graphite, polycrystalline Pt or Au, indium tin oxide on glass, or glassy carbon, by either horizontal or vertical transfer methods. LB film transfers with our trough required large sample sizes, and, as discussed above, the use of large amounts of C_{60} tended to lead to aggregation at the air/water interface. Because of the hydrophobic nature of C_{60}, better transfers could be made onto electrodes with more hydrophobic surfaces, i.e., alkyl thiol- or iodine-modified polycrystalline gold[37,38] or iodine-modified Pt single crystal.[39–41] These substrates afforded more reproducible film transfers than the bare unmodified substrates; it was possible to obtain routinely films of 2–5 layers thickness and, more rarely, monolayer films. However, for all of these films (1–5 layers) the electrochemical behavior observed was similar. A CV of a thin film of C_{60} on an octadecanethiol–gold modified electrode is shown in Figure 14. An important characteristic of this voltammogram is the presence of a much smaller peak splitting (150 mV peak to peak) than observed for thicker films. The reduction peaks were observed at about the same potential as for thicker films. The charge passed during the reoxidation (2.8 μC) was only about half of that during reduction (6.5 μC). This could be correlated to the observation of much smaller peak intensities during the following cycles. The surface coverage calculated from the charge passed during the first reduction process (integration of the first reduction peak) was 1.9×10^{-5} C/cm^2, which is equivalent to ~1.2 monolayers on the electrode. Similar CVs could also be obtained, although less frequently, in the absence of adsorbed thiols. Most of the results were obtained by a vertical transfer technique. In the vertical transfer mode, film transfer occurred only on substrate withdrawal through preformed films. The amount of material transferred decreased with decreasing transfer pressure. Monolayer films (as estimated from integration of the first reduction wave) were transferred only by withdrawing hydrophobic substrates through a preformed C_{60} film at 5–10 mN/m. The reproducibility of monolayer film transfer on unmodified substrates was very poor even at low transfer pressures. Independent of the substrate, films transferred at $\Pi > 30$ mN/m were not uniform but appeared visibly patchy with yellow clumps interspersed with large domains of clean substrate surface. We were unable to accumulate multilayer films by repetitive substrate dipping and withdrawal at low pressures, as surface material appeared to be lost on reimmersion of the substrate; similar flaking-off of cadmium stearate and other surfactant LB films upon substrate reimmersion into subphase has been found.[39] This difference in the electrochemical behavior can be explained by a better packing of the films when formed on the trough. The behavior observed for thick films in the presence of TBA^+ is due to the porosity and the loose structure of these films, which makes possible the incorporation of large molecules.

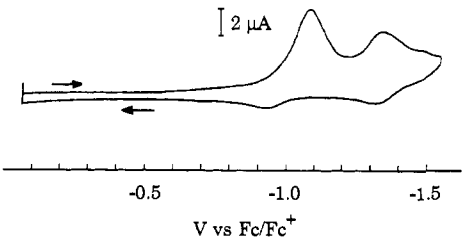

Figure 14. Cyclic voltammogram of LB film of C_{60} on an alkyl thiol–gold modified electrode (0.18 cm^2, gold sputtered on glass). The film was transferred vertically at 5 mN/m and presumably represents 1–2 monolayers. Supporting electrolyte, 0.1 M $TBABF_4$; scan rate, 200 mV/s.

The LB films were also characterized by contact angle (θ) measurements with water. The C_{60} patches were found to be very hydrophobic ($\theta \sim 100°$). Exposure of the immobilized C_{60} on any of the substrates to 3:1 H_2SO_4/H_2O_2, followed by copious water and EtOH washes and drying in Ar, did not remove the C_{60}. Contact angles on the C_{60} patches after such treatment were much lower ($\theta \sim 25°$), suggesting that the C_{60} surface had been oxidized and became more hydrophilic.

Preliminary experiments suggested that C_{60} could also be immobilized on a surface during the formation of self-assembled (SA) films onto a thiol-modified gold electrode. An electrode was immersed overnight in a solution of C_{60}/octadecanethiol (8:1) dissolved in benzene. After rinsing the electrode with benzene to remove any excess of C_{60}, a small peak for the first reduction of C_{60} was seen. Further experiments with LB and SA films are under way.

(34) Krätschmer, W.; Lamb, L. D.; Fostiropoulos, K.; Huffman, D. R. *Nature* **1990**, *347*, 354.
(35) (a) Miller, C. J.; Bard, A. J. *Anal. Chem.* **1991**, *63*, 1707. (b) Miller, C. J.; McCord, P.; Bard, A. J. *Langmuir* **1991**, *7*, 2781.
(36) *Physical Chemistry of Surfaces*, 3rd ed.; Adamson, A. W., Ed.; Wiley: New York, 1976; p 148.
(37) Miller, C. J.; Cuendet, P.; Grätzel, M. *J. Phys. Chem.* **1991**, *95*, 877.
(38) Miller, C. J.; Grätzel, M. *J. Phys. Chem.* **1991**, *95*, 5225.
(39) Rodriguez, J. F.; Soriaga, M. P. *J. Electrochem. Soc.* **1988**, *135*, 616.
(40) Bravo, B. G.; Michelbaugh, S. L.; Soriaga, M. P.; Villegas, I.; Suggs, D. W.; Stickney, J. L. *J. Phys. Chem.* **1991**, *95*, 5245.
(41) Deakin, M. R.; Li, T. T.; Melory, O. R. *J. Electroanal. Chem.* **1988**, *243*, 343.
(42) Okahata, Y.; Ariga, K. *Langmuir* **1989**, *5*, 1261.

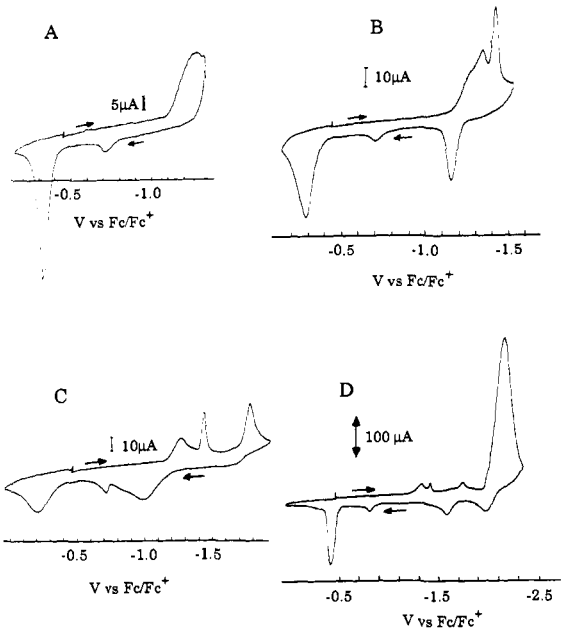

Figure 15. Cyclic voltammograms of C_{70} films on a gold electrode (2-mm diameter). Reduction reactions on the film: (A) scan over first reduction peak; (B) over second reduction; (C) over third reduction; (D) over fourth reduction. Supporting electrolyte, 0.1 M $TBABF_4$; scan rate, 200 mV/s.

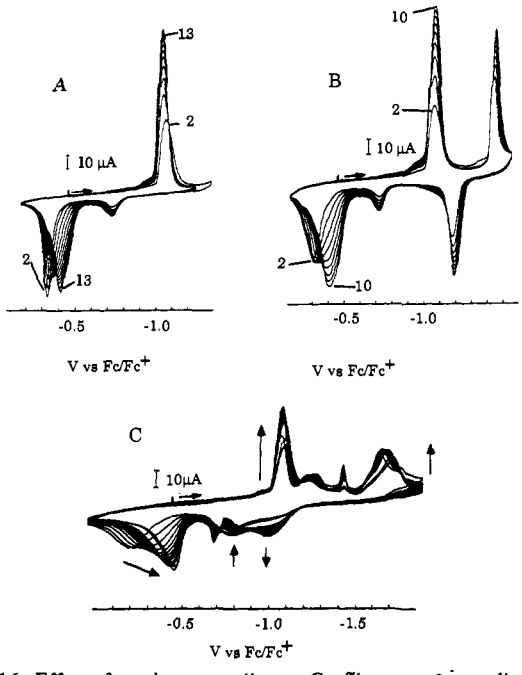

Figure 16. Effect of continuous cycling on C_{70} films on a 2-mm-diameter gold electrode. Supporting electrolyte, 0.1 M $TBABF_4$; scan rate, 200 mV/s. (A) Over first reduction wave; (B) over second reduction; (C) over third reduction. Numbers indicate cycle number and arrows indicate peak behavior with time.

Results: C_{70} Films

Cyclic Voltammetry. The same type of voltammetric experiments were performed on C_{70} films in MeCN with $TBABF_4$ as a supporting electrolyte. Typical voltammograms are shown in Figure 15. As with C_{60} films, C_{70} films showed four reductions with cathodic peak potentials at −1.26, −1.43, −1.77, and −2.16 V vs Fc/Fc^+. These peaks displayed generally similar behavior to that of C_{60} films. However, the separation between the cathodic peak potentials for the first and second reduction waves was larger than for the C_{60} system. A large splitting was still observed between the first reduction and reoxidation process, with ΔE_p somewhat larger than for the C_{60} films (750 vs 600 mV). The

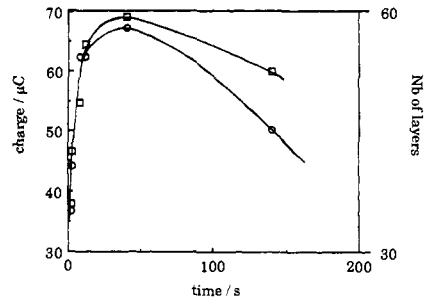

Figure 17. Charge calculated from the integration of the CV wave. (□) first reduction wave and (○) reoxidation wave. Right scale: number of layers reduced. The total number of layers on the electrode is close to 180.

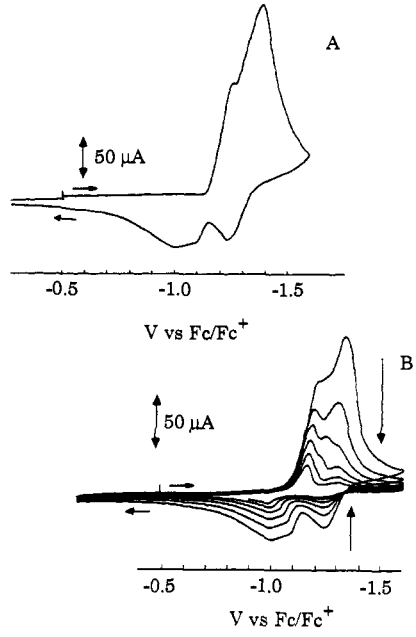

Figure 18. Cyclic voltammogram of C_{70} films on a 2-mm-diameter gold electrode in the presence of 0.1 M KPF_6 as supporting electrolyte. Scan rate, 200 mV/s. (A) First cycle; (B) following cycles.

peak splitting for the second reduction/reoxidation was similar to that observed for C_{60} (about 250 mV). The effect of continuous cycling is also quite different from that observed for C_{60} films (Figure 16). As with C_{60} films, the first reduction peak shifted (about 200 mV) toward more positive potentials between the first and the second cycle. A change in the shape of the reduction peak was also observed, suggesting reorganization of the film and perhaps the release of trapped solvent molecules. The charge calculated from the integration of the peak and compared to the amount of material on the surface showed that only about 25% of the material was reduced during the first scan, assuming a one-electron transfer. Upon continuous scanning, the peaks continued to grow until about 31% of the material was reduced. Figure 17 shows the variation of the charge in the film during the cycling over the first redox pair. Total one-electron reduction of the film never exceeded this 30% level on cycling. Upon further cycling, the peak currents started to decrease. The C_{70} films were more stable than the C_{60} films upon continuous cycling, since a longer cycling time was possible before suppression of the electrochemical activity appeared. Another difference compared to the C_{60} films was the shift of the first anodic peak upon continuous cycling. The anodic peak current first decreased then increased again with time while the peak potential shifted toward more negative values (Figure 16). The situation observed after 10–15 cycles was closer to the C_{60} case in terms of peak splitting, at least for the first reduction process.

Continuous cycling over the third reduction process also showed modifications of the CV with time. As opposed to the C_{60} system,

a pair of new peaks grew with time, while the anodic peak associated with the second reduction slowly decreased. Scanning the potential over the fourth reduction wave again irreversibly modified the CV, showing instability of the product of this reaction as observed for C_{60} films and dissolved C_{60} and C_{70}.[2,5-7]

C_{70} films were also studied in MeCN solutions containing a different supporting electrolyte, KPF_6 (Figure 18). Again the behavior was very different from that found with TBA^+. A split reduction wave was observed with two anodic waves on reversal, one at potentials near the cathodic wave and another split wave at more positive potentials. The charge associated with the anodic peak represents about 50% of the charge passed during the reduction compared to 40% found with TBA^+. Moreover, these films appear more stable upon continuous cycling compared to C_{60} films in KPF_6.

Langmuir Trough Experiments. The C_{70} films, deposited on the trough in the same manner as the C_{60} films, show two transitions in their Π–A isotherms (Figure 13C); the limiting areas yielded radii of 9.0 ± 3.0 and 5.8 ± 1.6 Å, respectively. These values are in reasonable agreement with the theoretical value expected for the prolate sheroidal C_{70} carbon cages in two configurations, i.e., the limiting areas corresponding to a film made up predominantly of C_{70} molecules with their long axis parallel to the interface at low pressures and one in which the molecules predominantly stand vertically at high pressures. Whereas the general features (e.g., film phase changes) in the C_{70} films were reproducible, a wider range of limiting areas was observed in replicate experiments, indicated by the standard deviations quoted. This is in marked contrast to the observations on the spherical C_{60} molecules. Mass spectroscopy of material recovered from the air/water interface after these experiments was the same as that of the original C_{70} material, showing that decomposition of the sample did not occur in these experiments. Furthermore, the C_{70} films formed bi- and multilayers more readily than the C_{60} films. These bi- and multilayers of C_{70} showed a single transition in their isotherms with $2.0 < r < 5.0$ Å. Extreme care had to be taken to form monolayer films that show the characteristic phase transitions; smaller sample sizes, slower sample application, effective temperature control, and slower rates of compression than were routinely used in the C_{60} studies had to be employed with the C_{70} films.

C_{70} also formed mixed films with arachidic acid, and these Π–A isotherms showed two transitions (Figure 13D). The limiting radius in the fully compressed film, $r \sim 7.8$ Å, suggests that, in contrast to the C_{60}–AA films, the C_{70} molecules in these films are much closer to the air/water interface and make significant contributions to the ultimate film packing. Like the C_{60}–AA films, these films also routinely survived $\Pi > 70$ mN/m, appeared to be solid at $\Pi \sim 30$ mN/m, and showed significant hysteresis upon expansion and recompression.

Conclusions

The results reported here indicate that the films cast from fullerene solutions in nonpolar solvents are porous and probably consist of C_{60} or C_{70} crystallites. Upon reduction in MeCN, TBA^+ or larger cations can penetrate into the crystallites with a large change in crystallite structure and the formation of a more compact film. The reduced material is slightly soluble in the MeCN; this solubility appears associated, at least to some extent, with solvent from the casting solution that remains in the film. The film can be reoxidized to recover the C_{60} or C_{70} structure. Although electrochemical transformation of fullerene and quaternary ammonium fulleride films is possible, neither are good electronic conductors. However, the conductivity and porosity of the films appears to be sufficient for almost complete reduction and reoxidation at slow scan rates. The partially reduced material, $(R_4N^+)_xC_{60}^{x-}$, where $0 < x < 1$, is a better conductor. The nature of the solution cation is important in the redox process, and different behavior is found with K^+ and Cs^+, which can enter the fcc C_{60} lattice. In this case a more reversible intercalation of the cation is suggested, but the reduced forms $M^+C_{60}^-$ appear to be much less stable, compared to R_4N^+ films. The processes occurring on reduction beyond the first electron transfer are less clear. Reduction at the second wave is less complete, perhaps because this structure is even more compact or resistive and less amenable to cation intercalation. Reduction at the third and fourth waves leads to irreversible loss in electroactivity of the film, as does oxidation. These large structural changes do not occur with monolayer or bilayer films prepared by the LB technique.

Langmuir trough studies with C_{60} or C_{70} at the air/water interface indicate relatively high incompressibility of the fullerene films. The high surface pressures sustained by monolayer films of both compounds suggest strong attractive interactions between the fullerene molecules with the formation of rigid films. These results agree with calculations and experiments which show that C_{60} crystals are much less compressible than graphite.[1b] Mixed films of the fullerenes with surfactants like arachidic acid can also be formed. In these films the fullerenes probably reside in the hydrocarbon environment of the surfactant tails.

Acknowledgment. We thank F. Wudl, K. C. Khemani, and A. Koch for supplying C_{60} and K. Kadish and D. Dubois for suggestions about film solubility. The support of this research by the National Science Foundation (CHE 8901450) and the Robert A. Welch Foundation is gratefully acknowledged.